First measurement of the -decay half-life of ^{206}Au

2015 EPL 111 52001

(http://iopscience.iop.org/0295-5075/111/5/52001)

A Letters Journal Exploring the Frontiers of Physics

September 2015

EPL, **111** (2015) 52001 www.epljournal.org
doi: 10.1209/0295-5075/111/52001

First measurement of the β-decay half-life of ^{206}Au

A. I. Morales[1,2], G. Benzoni[2], N. Al-Dahan[3], S. Vergani[1], Zs. Podolyák[4], P. H. Regan[4,5], T. P. D. Swan[4], J. J. Valiente-Dobón[6], A. Bracco[1,2], P. Boutachkov[7], F. C. L. Crespi[1,2], J. Gerl[7], M. Górska[7], S. Pietri[7], P. M. Walker[4] and H.-J. Wollersheim[7]

[1] *Università degli Studi di Milano - I-20133 Milano, Italy*
[2] *INFN, Sezione di Milano, I-20133 Milano, Italy*
[3] *Department of Physics, College of Science, University of Kerbala, Kerbala, Iraq*
[4] *Department of Physics, University of Surrey, Guildford, GU2 7XH, UK*
[5] *National Physical laboratory, Teddington, Middelsex, TW11 0LW, UK*
[6] *Istituto Nazionale di Fisica Nucleare, Laboratori Nazionali di Legnaro, Legnaro, Italy*
[7] *GSI Helmholtzzentrum für Schwerionenforschung, Darmstadt, Germany*

received on 24 August 2015; accepted by T. Hansl-Kozanecki on 31 August 2015
published online 10 September 2015

PACS 23.40.-s – β decay; double β decay; electron and muon capture
PACS 26.30.Hj – r-process
PACS 27.80.+w – $190 \leq A \leq 219$

Abstract – The β decay of the $N = 127$ isotone ^{206}Au has been investigated at the Gesellschaft für Schwerionenforschung laboratory within the rare isotope investigations at GSI Collaboration. From the experimental data, both its half-life and the level structure of the $N = 126$ daughter nucleus ^{206}Hg have been extracted. On the basis of the new results, the systematics of Au β-decay half-lives beyond the $N = 126$ shell closure is discussed. In addition, the interplay between allowed Gamow-Teller and first-forbidden transitions in the $N > 126$, $Z < 82$ mass region is reviewed.

Introduction. – During the last years a major progress has been achieved in the knowledge of shell properties in exotic nuclei far away from stability. The evolution of the shell structure in nuclear systems with large neutron-to-proton ratios is a key factor to understand, for instance, the breakdown of classic shell closures and the development of new energy gaps [1], or the coexistence of shapes in semi-magic nuclei [2]. These structural properties have an important impact on the astrophysical rapid-neutron capture process (r-process) of nucleosynthesis [3], whose pathway passes through very exotic neutron-rich nuclei from Ni to U through a series of rapid neutron captures and β decays. Both the abundance pattern and time scale depend strongly on the half-lives, Q_β energies, and β-delayed neutron emission probabilities of the r-process nuclei, and consequently, a precise knowledge of these quantities may help to understand better the astrophysical sites where the r-process might develop, as shown in recent sensitivity studies [4].

Within this framework, renewed interest has been conferred to the heavy region around $N \sim 126$, which is associated with the third r-process peak at $A = 195$ in the solar abundance distribution. A current question open to debate is the competition between allowed Gamow-Teller (GT) and first-forbidden (*ff*) decays in $N \sim 126$ nuclei. The particular ordering of the single-particle orbitals is expected to favor the appearance of very fast, *ff* β transitions in this mass region. These are expected to reduce significantly the theoretical lifetimes [5–8], increasing the flow of matter through the third r-process bottleneck and, consequently, the re-processing through fission. However, the β-decay studies reported thus far for $N > 126$ nuclei point to a smaller contribution of *ff* strength in some isotopic chains [9,10], at variance with the good agreement found in the $N < 126$, $Z < 82$ quadrant [11,12]. Recent attempts to synthesize $N \sim 126$ neutron-rich nuclei have been focused on the fragmentation of ^{208}Pb and ^{238}U projectiles [13–15] and on the relativistic charge exchange of ^{208}Pb [16]. Such progress has opened up the possibility of performing β-delayed γ spectroscopy of a few $N \sim 126$ nuclei close to ^{208}Pb [10,17–19]. In particular, in the $N > 126$, $Z < 82$ quadrant, the only β-decay information available belongs to moderately neutron-rich Tl and Hg isotopes [9,19,20]. Hence, the study of lighter $N > 126$ nuclei lying closer to the r-process path is of primary interest.

This letter reports on the investigation of ^{206}Au, the lightest $N = 127$ isotone for which β-decay data are presently available. Earlier studies on the daughter nucleus ^{206}Hg exploited α decay [21], transfer and deep-inelastic reactions [22–24], and fragmentation of relativistic heavy stable beams [25–27]. Here we report, for the first time, the half-life of ^{206}Au and the observation of a β-decay branch to the $J^\pi = 5^-$ isomer in ^{206}Hg. The new results are discussed in terms of the underlying nuclear structure and the possible appearance of allowed β transitions with the opening of the $N > 126$ major shell.

Experimental details. – The experiment was carried out at the Gesellschaft für Schwerionenforschung laboratory (GSI, Germany). A ^{238}U primary beam was delivered by the SIS-18 synchrotron with an energy of 1 GeV/nucleon and an average intensity of $5 \times 10^8\,\mathrm{s}^{-1}$. The nuclei of interest were produced in fragmentation reactions on a Be target 2.5 g/cm^2 thickness. The pulsed beam had two repetition cycles of 3 and 4 s with extraction times of 1 and 2 s, respectively. The identification of the nuclear species was performed in-flight in the high-resolution spectrometer fragment separator (FRS) through the Bρ-ΔE-Bρ method [28]. The nucleus ^{206}Au was selected in three magnetic settings centred in ^{205}Pt, ^{215}Pb, and ^{217}Pb. Standard FRS detectors, such as thin scintillators, time projection chambers, and ionization chambers were used to measure the horizontal position, time of flight, and energy loss of the nuclei throughout the spectrometer. The high energies reached by the SIS-18 synchrotron combined with the two-stage design of the FRS allowed for a clear separation of the different atomic charge states of the heavy nuclei following the procedure described in ref. [16].

The β decay of ^{206}Au was studied in a β-delayed spectroscopy setup located at the exit of the separator. The nuclei were decelerated in a homogeneous Al degrader before their implantation in the RISING (Rare ISotope INvestigations at GSI) active stopper, consisting of 6 double-sided silicon strip detectors (DSSSD) [29]. To illustrate the excellent identification of the implanted residues, mass identification matrices for the fully stripped nuclei in the final focal plane of the spectrometer and in the active stopper are shown in fig. 1. The wide dynamic energy range of the DSSSD pre-amplifiers allowed for a clear separation of implantation-, β-, and α-like signals. A total of 1073 implantation events of ^{206}Au were registered after summing up the statistics of the three FRS settings.

The high pixelation of the DSSSD array (each detector had 256 pixels with 9 mm^2 active area) allowed one to encode the time, x- and y-position of each type of signal on an event-by-event basis. This information was used in the off-line data analysis to define correlations in position and time in order to extract β-decay half-lives. Coincident γ-ray information was obtained with the RISING spectrometer set up in "stopped beam" configuration [30]. The β-γ correlation time window was set up to 100 μs, thus

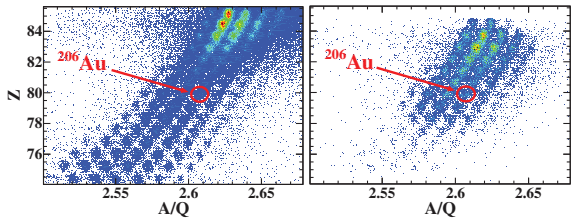

Fig. 1: (Color online) Particle identification matrices of the atomic number Z as a function of the mass-to-charge (A/Q) ratio for the FRS setting centred in ^{215}Pb. The left panel shows the total yields at the final focal plane of the separator, whereas the right panel displays the nuclei implanted in the active stopper. The ^{206}Au nuclei are delimited by red circles.

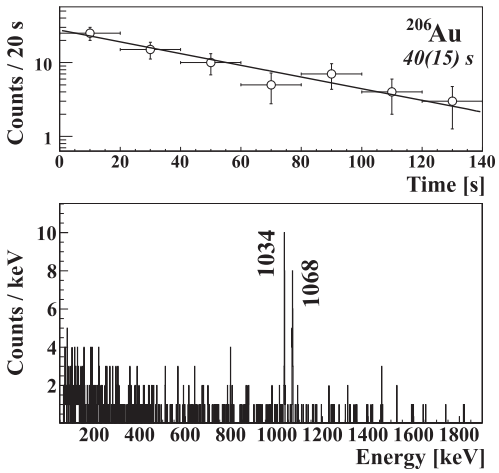

Fig. 2: Top: experimental time differences between implantations of ^{206}Au and delayed γ-rays of the daughter ^{206}Hg (empty circles). The fit to an exponential function is shown as a continuous line. Bottom: β-delayed γ spectrum of the decay ^{206}Au $\rightarrow$ ^{206}Hg extended to 5 half-life periods. The two transitions de-exciting the reported 5^- isomer in ^{206}Hg [22,26,27] are clearly visible.

enabling the measurement of half-lives of isomeric nuclear states with values ranging from several ns up to some ms.

Results. – The activity curve and β-delayed γ transitions of ^{206}Au are presented in fig. 2. They were extracted applying the delayed-coincidence technique, by defining a set of correlation conditions between implanted fragments, β decays, and coincident γ-rays. Details on this procedure are described in previous publications [9,10,19]. In the specific case of ^{206}Au, all β-like particles registered in and around the pixel of implantation were considered for analysis. In the corresponding β-delayed γ spectrum —shown in the bottom panel of fig. 2— two peaks at 1034 and 1068 keV are clearly visible. They were identified in previous publications as de-exciting the $t_{1/2} = 2.09(2)\,\mu$s, $J^\pi = 5^-$ isomer in the daughter ^{206}Hg [22,23,25–27]. The population of the metastable state further simplifies the extraction of the β half-life of ^{206}Au, since one can tag the β electrons with the delayed γ-rays of ^{206}Hg.

By applying this condition, contamination from δ electrons or other accidental β particles is easily suppressed, and the β electrons recorded during the beam spills can also be included in the analysis.

The upper panel of fig. 2 shows the time-correlated spectrum of ^{206}Au including the time differences between implantations and β particles in coincidence with delayed γ transitions of ^{206}Hg (empty circles). No contributions from background or decay chain descendants have been considered in the fitting procedure due to the high selectivity of the delayed γ-ray coincidence tag. Thus, the fit shown in the figure includes a single exponential-time distribution function describing the decay time behavior of ^{206}Au. The binned maximum likelihood (MLH) method has been applied due to the scarce statistics. The uncertainty of the measurement is calculated as the sum of statistical and systematic errors. The latter are related to the binning and correlation time window of the spectrum. The resulting half-life value is $t_{1/2} = 40(15)$ s.

Discussion. – Previous experiments reported the existence of two isomeric states in ^{206}Hg. The 2102 keV level was firstly observed in a ^{204}Hg(^{18}O, ^{16}Oγ)^{206}Hg reaction [31]. The state de-excited to the 2^+ level at 1068 keV emitting a γ-ray of 1034 keV. Due to the prompt character of this γ transition, the authors claimed a spin-parity $J^\pi = 4^+$ for the 2102 keV state. However, subsequent studies exploiting ^{204}Hg(t, γ)^{206}Hg reactions reported a half-life of 2.15(21) μs, and a final $J^\pi = 5^-$ was assigned [22,23]. This picture was in excellent agreement with shell-model calculations including the proton-hole interaction of ref. [32]: A dominant $\pi d_{3/2}^{-1} h_{11/2}^{-1}$ configuration was predicted for the first 2^+ state, while the next calculated level was a $J^\pi = 5^-$ state with a strong $\pi s_{1/2}^{-1} h_{11/2}^{-1}$ single-particle contribution.

The second isomer is located at 3723 keV and has a half-life of $t_{1/2} = 92(8)$ ns. It was firstly observed in deep-inelastic heavy-ion reactions [24] and more recently in relativistic fragmentation of heavy stable beams [25–27]. It has been interpreted as the (10^+) state arising from the fully aligned configuration $\pi h_{11/2}^{-2}$.

Partial level schemes of ^{206}Hg including states reported in the literature and the ones observed here are shown in fig. 3. It is worth noting that the maximum Q_β energy for the decay of ^{206}Au is calculated at 6700(300) keV [20]. Our measurement, then, is most likely affected by the pandemonium effect [33] and no absolute β intensities or log ft values are given for caution. But a tentative discussion based on the intensity balance of the observed γ-rays is still of interest. The relative intensity of the 1034 keV peak after correcting for γ efficiency is $I_\gamma = 320(50)$ arbitrary units, while that of the 1068 keV peak results in $I_\gamma = 290(50)$ arbitrary units. This indicates that the ground state of ^{206}Au preferentially decays to the yrast 5^- level in ^{206}Hg, with no direct feeding to the first 2^+ state. The rest of the transitions shown in the left part of fig. 3 are not observed in this β-decay work. These observations

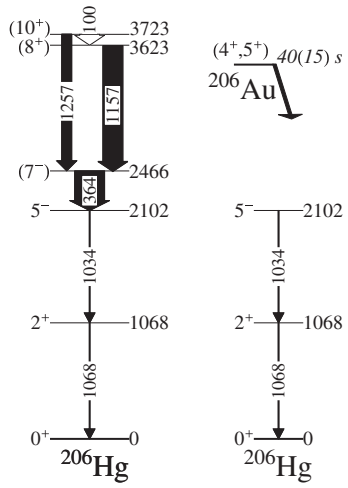

Fig. 3: Partial level schemes of ^{206}Hg. The left part shows low-lying yrast states reported in the literature [22,23,25–27]. The right part shows the levels populated in the present work, following β decay of ^{206}Au.

are in line with the ocurrence of a first-forbidden transition from the $J^\pi = (4^+, 5^+)$ ground state of ^{206}Au [34], which is expected to have as main single-particle configuration $\pi s_{1/2}^{-1} \nu g_{9/2}^{1}$.

In fig. 4 we show measured and theoretical half-lives for the neutron-rich isotopic chains of Tl and Au. With the inclusion of the newly measured value of ^{206}Au, the experimental trend is extended across the $N = 126$ shell closure for $Z = 79$. This allows one to perform a first comparative test of β-decay nuclear models in the $N > 126$, $Z < 82$ mass region. For simplicity, two theoretical predictions are considered here. These are the FRDM + QRPA approach (solid line) [35] and the DF3 + cQRPA theory [5] (dashed line). The first model is extensively used in calculations of r-process nucleosynthesis. Nevertheless, it was shown to overestimate significantly the half-lives of many $N < 126$ nuclei [11,12], and, to a lesser extent, the half-lives of nuclei near the $A \sim 80$ and 130 waiting points [36–39]. Such discrepancies are thought to occur due to an underestimation of the *ff* strength, which is calculated in the macroscopic framework of the statistical gross theory. This treatment might not be sufficient as *ff* transitions are expected to influence the β spectrum of many neutron-rich nuclei, especially in the $N \sim 126$ region where the *ff* strength is predicted to exceed the GT contribution [5–8].

The second model includes GT and *ff* transitions in the continuum Quasi-Particle Random-Phase Approximation (cQRPA), while the ground-state properties are calculated within the Fayans energy-density functional DF3. In general, the microscopic treatment of *ff* transitions brings the calculated half-lives closer to experiment [5–8], although for the $N > 126$ Tl isotopes the predictions of the FRDM + QRPA model reproduce better the experimental results [9]. It has been suggested that the allowed $(0i_{11/2}, 0i_{13/2})$ single-particle transition might be

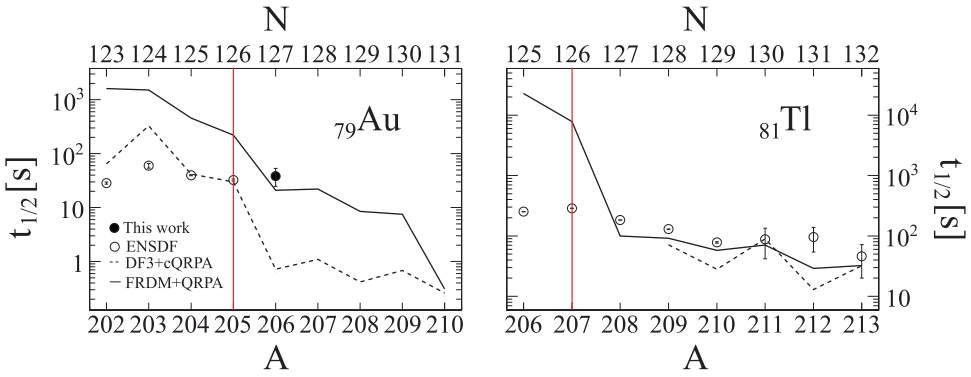

Fig. 4: (Color online) Experimental and theoretical half-lives as a function of the mass number A (bottom axis) and neutron number N (top axis) for Au (left) and Tl (right) isotopes. FRDM + QRPA predictions [35] are indicated as a continuous line, DF3 + cQRPA calculations [5] as a dashed line, previously measured half-lives [20] as empty circles, and the new experimental result as a filled circle. The $N = 126$ shell closure is indicated with a red line.

the leading component in the β decay of these nuclei [19]. This argument is based on shell-model calculations allowing one proton excitation across the $Z = 82$ shell closure, which predict an important fragmentation of the $\pi 0i_{11/2}$ orbital over several low-lying states in the daughter Pb isotopes, and an occupation of nearly one for the $\nu 0i_{11/2}$ orbital in the Tl ground states. This clearly favors the occurrence of the allowed decay.

Looking at fig. 4, the systematics at $N \leq 126$ are significantly overestimated by the FRDM + QRPA approach. These are better reproduced by the DF3 + cQRPA theory, in line with the expected larger contribution of *ff* strength to the total decay rates [5–8]. In general, both models predict a decreasing trend of the Au half-lives with the calculated values differing more than one order of magnitude up to ^{209}Au. Note that the downward trend of the theoretical predictions is enhanced for the $N = 127$ isotones (^{208}Tl and ^{206}Au). This is consistent with the gain in Q_β energy due to the presence of a neutron above the $N = 126$ shell gap. Nevertheless, the newly measured half-life of ^{206}Au is very similar to that of the $N = 126$ isotone ^{205}Au, defining an unexpected flat trend after the magic shell that is also observed in the isotopic chain of Tl. This behavior, which is independent of the large experimental uncertainty, has been previously reported in $N \geq 82$ nuclei below the $Z = 50$ proton shell closure [40]. Here, the absence of the deep kink in the half-life systematics has been correctly predicted by the DF3 + cQRPA theory [41], and is attributed to the occurrence of the allowed GT transition $\nu 0g_{7/2} \rightarrow \pi 0g_{9/2}$. This decay populates excited states in the daughter nuclei, as reported in ref. [42] and in the references therein. As a result, the increase in Q_β energy is not evinced by a sudden drop of the $N \geq 82$ half-lives. In the $N \sim 126$ region, the main GT transition mediating the β decay, $\nu 0h_{9/2} \rightarrow \pi 0h_{11/2}$, is highly blocked by the low transition energy and the partial filling of the $\pi h_{11/2}$ orbital [5]. Hence, the flat trend observed in fig. 4 might not be ascribed to the occurrence of allowed transitions from inner, fully occupied neutron sub-shells, as in the case of the $N \geq 82$ region. Additional justification comes from the striking underestimation of the DF3 + cQRPA half-lives for $N \geq 126$ nuclei [9,19]. In particular, for ^{206}Au, the experimental result exceeds by more than a factor 60 the theoretical prediction.

As anticipated above and in ref. [19], a plausible explanation for the unexpectedly slow decay rates would involve an increase in the occupation number of the $\nu 0i_{11/2}$ orbital. This is in line with the predictions of recent mean-field approaches [43], which find in the enhanced occupation of this orbital the origin of the anomalous kink observed in the charge radius isotope shift across the $N = 126$ shell gap. Though the physical mechanisms leading to a larger occupation of the $\nu 0i_{11/2}$ sub-shell have not been clearly determined, yet, several factors have been suggested as possible sources. Among them, a weakening of the spin-orbit field, which would reduce the energy splitting between the $g_{9/2} - g_{7/2}$ neutron spin-orbit partners. This would reduce the spacing —or even invert the ordering— of the $\nu 1g_{9/2}$ and $\nu 0i_{11/2}$ orbitals. Experimentally, they are separated by only ~ 800 keV [44,45]. This low-energy level difference might be subject to variations when removing protons from the closed shell. One well-known mechanism altering the single-particle energies is the tensor force [46], which has shown to induce rapid changes in the shell structure of lighter exotic nuclei [47]. In the heavy and super-heavy mass regions, the tensor force is expected to have also a significant effect on the spin-orbit splitting and shell evolution, see, for instance, refs. [48,49]. In the recent theoretical study on the proton bubble structure in ^{206}Hg [49], inclusion of the tensor force results in an inversion of the $\pi 2s_{1/2}$ and $\pi 0h_{11/2}$ orbitals when using the $SLy5 + T_w$ interaction, which has shown to reproduce well the spin-dipole experimental data in ^{208}Pb [50]. If this were the case, the proton-neutron tensor force between the $\pi 0h_{11/2}$ and the $\nu 1g_{9/2}, \nu 0i_{11/2}$ orbitals could induce an approach, or even an inversion, of the $\nu 1g_{9/2} - \nu 0i_{11/2}$ sub-shells in $N > 126$ nuclei below ^{208}Pb. As a result, the allowed

transition $\nu 0i_{11/2} \rightarrow \pi 0i_{13/2}$ could compete with the *ff* decay $\nu 1g_{9/2} \rightarrow \pi 0h_{9/2}$. The observation of a single decay branch to the 5^- state in ^{206}Hg disagrees with this assumption, yet its real feeding might be screened by undetected γ transitions from higher-lying states, which are difficult to measure given the scarce statistics and the use of HPGe detectors for the detection of γ transitions.

In conclusion, the unique capabilities of the FRS + RISING setup were exploited to investigate the β decay of ^{206}Au to ^{206}Hg, the lightest $N = 127$ isotone for which β decay spectroscopy has been performed. A unique β-decay branch to the reported 5^- isomer in ^{206}Hg has been observed, though this measurement is more likely to be affected by unobserved higher-lying feeding. The half-life of ^{206}Au has been reported, and a systematic comparison with theoretical predictions has shown an unexpectedly smooth trend across the $N = 126$ shell closure, suggesting the appearance of new shell effects beyond $N = 126$. The possible impact of the tensor force on the $\nu g_{9/2} - \nu g_{7/2}$ spin-orbit splitting and on the modification of the $\pi 0h_{11/2} - \pi 2s_{1/2}$ and $\nu 1g_{9/2} - \nu 0i_{11/2}$ single-particle energy spacings has been discussed. With the advent of the new generation of radioactive ion beam facilities, the β decay of this and lighter $N = 127$ nuclei will be studied with improved conditions.

* * *

This work was supported by Programmi di Ricerca Scientifica di Rilevante Interesse Nazionale (PRIN) No. 2010T24324_01302. The authors acknowledge the support of the Italian INFN and the STFC and EPSRC (UK). The excellent work of the RISING Collaboration and the GSI accelerator staff is also acknowledged.

REFERENCES

[1] Sorlin O. and Porquet M.-G., *Prog. Part. Nucl. Phys.*, **61** (2008) 602.
[2] Heyde K. and Wood J. L., *Rev. Mod. Phys.*, **83** (2011) 1467.
[3] Burbidge E. M., Burbidge G. R., Fowler W. A. and Hoyle F., *Rev. Mod. Phys.*, **29** (1957) 547.
[4] Surman R., Mumpower M., Cass J., Bentley I., Aprahamian A. and McLaughlin G. C., *EPJ Web of Conferences*, **66** (2014) 07024.
[5] Borzov I. N., *Phys. At. Nucl.*, **74** (2011) 1435.
[6] Suzuki T. *et al.*, *Phys. Rev. C*, **85** (2012) 015802.
[7] Zhi Q. *et al.*, *Phys. Rev. C*, **87** (2013) 025803.
[8] Fang D.-L., Brown B. A. and Suzuki T., *Phys. Rev. C*, **88** (2013) 034304.
[9] Benzoni G. *et al.*, *Phys. Lett. B*, **715** (2012) 293.
[10] Morales A. I. *et al.*, *Phys. Rev. C*, **88** (2013) 014319.
[11] Morales A. I. *et al.*, *Phys. Rev. Lett.*, **113** (2014) 022702.
[12] Kurtukián-Nieto T. *et al.*, *Eur. Phys. J. A*, **50** (2014) 135.
[13] Alvarez-Pol H. *et al.*, *Phys. Rev. C*, **82** (2010) 041602.
[14] Kurtukián-Nieto T. *et al.*, *Phys. Rev. C*, **89** (2014) 024616.
[15] Steer S. *et al.*, *Phys. Rev. C*, **78** (2008) 061302.
[16] Morales A. I. *et al.*, *Phys. Rev. C*, **84** (2011) 011601.
[17] Alkhomashi N. *et al.*, *Phys. Rev. C*, **80** (2009) 064308.
[18] Al-Dahan N. *et al.*, *Phys. Rev. C*, **85** (2012) 034301.
[19] Morales A. I. *et al.*, *Phys. Rev. C*, **89** (2014) 014324.
[20] `http://www.nndc.bnl.gov/ensdf/`.
[21] Kaunaren P., *Ann. Acad. Sci. Fenn., Ser. A VI*, No. 96 (1962).
[22] Becker J. A., Carlson J. B., Anier R. G. I., Mann L. G., Struble G. L., Maier K. H., Ussery L., Stöffl W., Nail T., Sheline R. K. and Cizewski J. A., *Phys. Rev. C*, **26** (1982) 914.
[23] Maier K. H., Menningen M., Ussery L. E., Nail T. W., Sheline R. K., Becker J. A., Decman D. J., Lanier R. G., Mann L. G., Stöffl W. and Struble G. L., *Phys. Rev. C*, **30** (1984) 1702.
[24] Fornal B. *et al.*, *Phys. Rev. Lett.*, **87** (2001) 212501.
[25] Pfützner M. *et al.*, *Phys. Rev. C*, **65** (2002) 064604.
[26] Steer S. *et al.*, *Phys. Rev. C*, **84** (2011).
[27] Al-Dahan N. *et al.*, *Phys. Rev. C*, **80** (2009).
[28] Geissel H. *et al.*, *Nucl. Instrum. Methods B*, **70** (1992) 286.
[29] Kumar R. *et al.*, *Nucl. Instrum. Methods A*, **598** (2009) 754.
[30] Pietri S. *et al.*, *Nucl. Instrum. Methods B*, **261** (2007) 179.
[31] Hering W. R., Puchta H., Trautmann W., McGrath R. L. and Bohn H., *Phys. Rev. C*, **14** (1976) 1451.
[32] Rystroem L. *et al.*, *Nucl. Phys. A*, **512** (1990) 217.
[33] Hardy J. *et al.*, *Phys. Lett. B*, **71** (1977) 307.
[34] Möller P., Nix J. and Kratz K.-L., *At. Data Nucl. Data Tables*, **66** (1997) 131.
[35] Möller P., Pfeiffer B. and Kratz K.-L., *Phys. Rev. C*, **67** (2003) 055802.
[36] Nishimura S. *et al.*, *Phys. Rev. Lett.*, **106** (2011) 052502.
[37] Arndt O. *et al.*, *Phys. Rev. C*, **84** (2011) 061307.
[38] Madurga M. *et al.*, *Phys. Rev. Lett.*, **109** (2012) 112501.
[39] Xu Z. *et al.*, *Phys. Rev. Lett.*, **113** (2014) 032505.
[40] Lorusso G. *et al.*, *Phys. Rev. Lett.*, **114** (2015) 192501.
[41] Borzov I., Cuenca-García J., Langanke K., Martínez-Pinedo G. and Montes F., *Nucl. Phys. A*, **814** (2008) 159.
[42] Taprogge J. *et al.*, *Phys. Rev. C*, **91** (2015) 054324.
[43] Goddard P. M., Stevenson P. D. and Rios A., *Phys. Rev. Lett.*, **110** (2013) 032503.
[44] Grawe H., Langanke K. and Martínez-Pinedo G., *Rep. Prog. Phys.*, **70** (2007) 1525.
[45] Chen J. and Kondev F., *Nucl. Data Sheets*, **126** (2015) 373.
[46] Otsuka T., Suzuki T., Fujimoto R., Grawe H. and Akaishi Y., *Phys. Rev. Lett.*, **95** (2005) 232502.
[47] Tsunoda Y. *et al.*, *Phys. Lett. B*, **89** (2014) 031301.
[48] Suckling E. B. and Stevenson P. D., *EPL*, **90** (2010) 12001.
[49] Wang Y. Z., Hou Z. Y., Zhang Q. L., Tian R. L. and Gu J. Z., *Phys. Rev. C*, **91** (2015) 017302.
[50] Bai C. L., Zhang H. Q., Sagawa H., Zhang X. Z., Colò G. and Xu F. R., *Phys. Rev. Lett.*, **105** (2010) 072501.